1. INTRODUCTION

Mixed convection is a coexistence of both Natural and Forced convection. The condition of flow in the natural state is buoyancy-driven. The side vent of the cavity contributes to the intake of airflow, hence exhibiting complex airflow patterns. Due to a buoyancy difference through the cavity, there exists a pressure differential between the intake air at an ambient temperature from the side vent and the air at a different temperature due to a constant heat source. This pressure differential causes hot air to move away from the heat source through the energy absorbed and then releases this energy as heat. This flow of heat is called Natural Convection. Natural convection is also accompanied by Forced convection. Under Forced convection, the airflow is caused by an external force. This force is usually in terms of a fan. This fan is supplied with a constant energy supply to give a uniform velocity to the airflow. This airflow, when passing through a temperature gradient of the cavity, causes the transfer from the ambient air to the hotter air; the hotter air then rises and thus releases the energy as heat, and the cycle continues. When these two convections coexist and occur simultaneously in a system with a constant heat source and a constant velocity air supply, the system experiences Mixed Convection.

In environmental investigations, Natural and Forced ventilation are often studied separately, providing clear insights into their impacts. However, their interaction becomes crucial in real-world scenarios where external air circulation meets internal heating systems. For example, the central processing unit (CPU) has an advanced ventilation system with strategically positioned cooling fans in a personal computer. As the CPU processes data, it generates significant heat, which can lead to malfunctions if not managed properly. The ventilation system draws in cooler air while the fans create airflow to expel hot air, maintaining a safe operational temperature. This combined approach of Natural and Forced ventilation is essential for enhancing performance and protecting the device from overheating, thereby ensuring its longevity and reliability.

This research provides a comprehensive exploration of the intricate dynamics of airflow within thermodynamic systems, employing a blend of experimental methodologies and advanced numerical simulations. It delves into the mechanisms of heat transfer, meticulously investigating how various factors—such as temperature gradients, the aspect ratios of cavities and heat sources, and airflow rates—impact overall performance. By applying these insights, we can optimize the design and functionality of air cavities tailored for a wide array of modern applications, significantly reducing the risk of overheating that can compromise device reliability and efficiency. Additionally, the findings contribute to the design of living spaces that prioritize comfort, facilitating effective indoor temperature regulation. This not only enhances the overall quality of life for occupants but also promotes energy efficiency, making these solutions beneficial for both residential and commercial settings. Ultimately, this research paves the way for innovative designs that marry functionality with user comfort in an increasingly complex technological landscape.

This research thoroughly investigates the intricate dynamics of buoyancy-driven mixed convection occurring in side-vented cavities. It examines how natural convection, which is driven by buoyancy forces due to temperature differences, interacts with forced convection, where fluid motion is induced by external means such as fans or pumps. By analyzing these two convection mechanisms, the study aims to enhance the understanding of their combined effects on heat transfer and fluid flow patterns. The findings are intended to provide valuable data and refined modelling approaches that can be applied in various engineering contexts, improving efficiency and performance in systems that rely on effective thermal management.

2. Review of Literature

Raji and Hasnaoui[i] [2001] analyzed 2-D steady, laminar mixed convection heat transfer in an air-filled rectangular cavity with vents, focusing on Rayleigh numbers from 10^3 to 5×10^6, emissivity from 0.0 to 1.0, and Reynolds numbers from 50 to 5000. Using the finite difference method to discretize the vorticity-stream function form of the Navier-Stokes equations, the results revealed the notable impact of thermal radiation on temperature distribution, fluid flow, and heat dissipation across the cavity's active walls.

Bahlaoui et al.[ii] [2011] studied mixed convection in an air-filled, adiabatic vented enclosure with uniform heat flux. They analyzed Reynolds numbers from 200 to 5000 and emissivity from 0.0 to 1.0, as well as varying baffle positions and heights. Using the finite difference method, they found that heat dissipation significantly depended on vent location and baffle height.

Venkatachalapathy and Udayakumar[iii] [2012] investigated mixed convection in a cavity with a 5×4 array of protruded heat sources on the bottom wall through numerical and experimental methods, using FLUENT 6.3 for simulations.

Belmiloud et al.[iv] [2017] numerically studied the effect of baffle length ($L = 0.3$ to 0.7) on mixed convection heat transfer in a rectangular vented enclosure with a heated inner wall under uniform heat flux. Using the FDM and SIMPLE algorithm with the Boussinesq approximation, they analyzed conditions for $Pr = 0.71$, $50 \leq Re \leq 500$, emissivity, $0.0 \leq \varepsilon \leq 0.15$, Grashof's number, $Gr^* = 104$, and the baffle length as $L = 0.3$ to 0.7. The study found that increasing baffle length enhances the total Nusselt number.

Doghmi et al.[v] [2018] numerically studied mixed convection in a 3D vented enclosure with an isothermal heat source, using FVM to analyze the effects of port locations 50 ≤Re ≤100, and 0 ≤Ri ≤10. Optimal parameter choices enhanced flow and cooling efficiency.

Prasad et al.[vi] [2019] simulated laminar natural convection and surface radiation (ε =0.05–0.85) for air (Pr =0.70) in 2D open enclosures. Using finite volume techniques under Boussinesq approximation, they analyzed parameters like aspect ratio 1 ≤A ≤2, vent - port ratio, 0.25–1, and Rayleigh number, 104 ≤Ra*≤107. Optimal heat source and vent locations enhanced cooling efficiency.

Prakash and Singh[vii][2022] investigated steady laminar mixed convection and surface radiation in an air-filled enclosure with constant heat flux on the vent side. Experiments cover Q =3.19 W–16.71 W, Reynolds number, Re =4814–166385, and Richardson number, Ri =0.1–25. Numerical simulations, performed for, A =1–5, and surface emissivity, ε =0.05–0.85 solve the momentum and energy equations via the finite-volume method using a Fortran 90 code. Correlations for Nusselt number and maximum surface temperature are derived from experimental data.

Based on these interpretations, this study focuses on mixed convection flow and surface radiation in a vented enclosure with constant heat flux on the vent side, considering parameters like Reynolds number, Richardson number, aspect ratio, and emissivity. Although such a geometry may not frequently occur with a single heat source, it provides a foundation for analysing more complex systems with multiple heat sources. The study combines both numerical and experimental methods to examine the flow regimes in natural, forced, and mixed convection.

3. <u>Experimental Setup and Procedure</u>

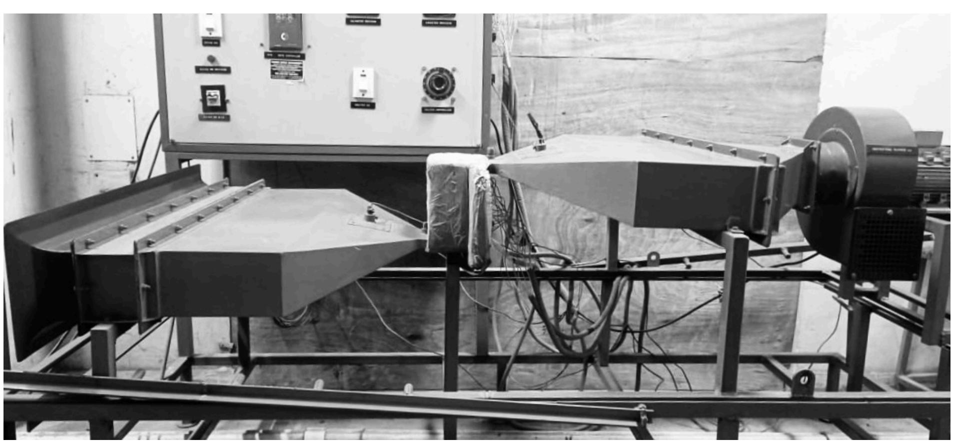

Figure 1 – Experimental Setup

3.1 Side-vented Cavity

Structure

The structure is a rectangular entity with an internal cavity of 200 mm by 100 mm, equipped with an air inlet at the base and an outlet at the top to facilitate airflow. This design is vital for applications in fluid dynamics and thermal management, where effective airflow control is essential for system performance.

Material

A robust heating apparatus, measuring 180 mm by 150 mm, is equipped with a mica casing to deliver accurate thermal flux to designated surfaces. All sides of the enclosure, except for the vented side, are insulated with 20 mm thick Hylum sheets. The chamber's frame is constructed using a 2 mm thick mild steel (MS) sheet. The joints between the Hylum sheets are sealed with Teflon tape, ensuring an adiabatic boundary to prevent heat loss and fluid leakage.

Figure 2 – Side Vented Cavity

Heating Element

A 180 mm x 150 mm heating element, encapsulated by a mica sheet, provides regulated heat flux to targeted surfaces. This design allows for uniform or localized heating tailored to the experimental objectives, ensuring precise thermal management for optimal outcomes.

3.2 Air-Flow System

Air Blower

The study investigates the forced convection phenomenon, with regulation achieved through a variable frequency drive that modulates airflow rates. This approach allows for precise control of the convection process, facilitating a comprehensive analysis of its effects under varying conditions.

Settling Chambers

The structure, 240mm x 120mm x 2mm, is designed with honeycomb structures and mesh filters, which serve to regulate airflow uniformly and mitigate turbulence before entering the experimental section.

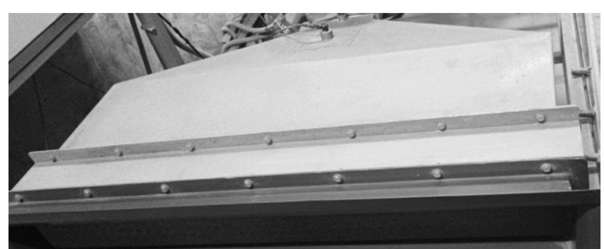

Figure 3 – Air Blower Component

Nozzle

The airflow is directed into the cavity, ensuring the maintenance of consistent and uniform velocity profiles throughout the medium.

Suction Chamber

Facilitates airflow extraction with low velocity to maintain smooth flow profiles.

3.3 Measurement Instruments

Thermocouples

Accurate temperature measurement at various points on heated surfaces, as well as in inlet and outlet passages and cavity walls, is essential for effective thermal management. Typically, fifteen K-type thermocouples are placed in a 5 x 3 configuration on heating elements to determine the average heated temperature, while fourteen thermocouples on the surrounding walls calculate the average ambient temperature. K-type thermocouples are preferred for their exceptional accuracy and wide temperature range, making them ideal for thermal analysis applications.

Wattmeter

Voltage and current are monitored using a DC power supply with a voltmeter and ammeter to calculate heat input.

Anemometer

Measures inlet airflow velocity for calculating Reynolds number and airflow characteristics.

Emmisometer

Emissivity ranging from 0 to 1 of the heating element is measured by this.

3.4 Experimental Procedure

- The emissivity of the heating surface is noted using an Emmisometer.
- The power supply to the system is given by adjusting the voltage.
- The blower is turned on, adjusting the air velocity.
- Once the steady state is achieved, voltage, current, air velocity, and temperature readings are noted.

4. Data Reduction

Input Power: $Q = V \cdot I$ ………………………………………………………………………… (i)

Heat Losses: $Qcv = Q - Qrd - Qcond - Qside - Qenv - Qcontact - Qthermocouple$…(ii)

Heat Flux: $q' = \frac{Qcv}{As}$………………………………………………………………………...(iii)

Radiative Heat Loss: $Q_{rd} = \epsilon\sigma A_s\left({T_{avg}}^4 - {T_w}^4\right)$……………………………………………(iv)

Grashof's Number: $Gr = \frac{g\beta\Delta TL3}{\nu 2}$…………………………………………………………...(v)

Nusselt Number: $Nu_{cv} = \frac{Q_{cv}L}{A_s\Delta Tk_f}$……………………………………………………...(vi)

Reynolds Number: $Re = \frac{u_\infty L}{v}$……………………………………………………........(vii)

Non-Dimensional Temperature: $\phi = T_{avg} - \frac{T_\infty}{\Delta T_{ref}}$……………………………………...(viii)

Modified Grashof's Number: $Gr^* = \frac{g\beta q'L^4}{k_f\nu^2}$…………………………………………...(ix)

Rayleigh Number: $Ra^* = Gr^* \cdot Pr$………………………………………………………(x)

Richardson Number: $Ri^* = Gr^* \cdot Re^2$……………………………………………………...(xi)

5. <u>Numerical Investigation</u>

5.1 <u>Assumptions</u>

- Density variations are negligible.
- The flow is assumed to be steady and laminar.
- The fluid (air or another cooling medium) is treated as incompressible with constant properties.
- The heating element provides a constant heat flux or temperature.
- The surrounding walls are adiabatic.
- Velocity and temperature at the inlet are assumed to be uniform.
- The effects of viscous dissipation on the energy equation are neglected.
- A 2D simulation is considered to reduce computational complexity, assuming negligible variation in the third dimension.
- Surface radiation is modeled using emissivity values and the Stefan-Boltzmann law.

5.2 Dimensionless Variables

$$U = \frac{u}{u_\infty}, V = \frac{v}{u_\infty}, X = \frac{x}{L}, Y = \frac{y}{L}, P = \frac{p}{\rho u_\infty^2}, \Theta = \frac{T - T\infty}{(T_H - T\infty)}, \tau = \frac{tu_\infty}{L}$$

5.3 Governing Equations

Continuity Equation: $\frac{\partial U}{\partial X} + \frac{\partial V}{\partial Y} = 0$……………………………………………………………(xii)

Navier-Stokes Equation:

- X-momentum: $U\frac{\partial U}{\partial X} + V\frac{\partial V}{\partial Y} = -\left(\frac{\partial P}{\partial X}\right) + \left(\frac{1}{Re}\right)\left(\frac{\partial^2 U}{\partial X^2} + \frac{\partial^2 U}{\partial Y^2}\right)$………………………………...(xiii)
- Y-momentum: $\frac{\partial V}{\partial \tau} + U\frac{\partial V}{\partial X} + V\frac{\partial V}{\partial Y} = -\frac{\partial P}{\partial Y} + \left(\frac{1}{Re}\right)\left(\frac{\partial^2 V}{\partial X^2} + \frac{\partial^2 V}{\partial Y^2}\right) + Ri * \theta$……………………(xiv)

Energy Equation: $U\frac{\partial \theta}{\partial X} + V\frac{\partial \theta}{\partial Y} = \left(\frac{1}{Re.Pr}\right)\left(\frac{\partial^2 \theta}{\partial X^2} + \frac{\partial^2 \theta}{\partial Y^2}\right)$…………………………………...................(xv)

5.4 Dimensionless Boundary Conditions

Velocity:

- Inlet: $U = 1, V = 0$…………………………………………………….……………………(xvi)
- Outlet: $\frac{\partial U}{\partial X} = 0, \frac{\partial V}{\partial X} = 0$……………………………………………………………………...(xvii)
- Walls: $U = 0, V = 0$ $(No - slip\ boundary\ condition)$…………………………………(xviii)

Temperature:

- Inlet: $\theta = 0$……………………………………………………………………………….(xix)
- Heated Wall: $q'' = -\frac{\partial \theta}{\partial X}$……………………………………………………………………(xx)
- Adiabatic Walls: $\frac{\partial \theta}{\partial n} = 0$…………………………………………………………………(xxi)

5.5 Richardson Impact

The Richardson number (Ri) determines the dominance of natural versus forced convection:

- Ri≪1: Forced convection dominates.
- Ri≫1: Natural convection dominates.
- Ri≈1: Mixed convection regime.

6. **Future Scope**

6.1 Model Data

Power Input (W)	Air Velocity (m/s)	Heated Temp 1	Heated Temp 2	Heated Temp 3	Heated Temp 4	Heated Temp 5	Heated Temp 6	Heated Temp 7	Heated Temp 8	Heated Temp 9	Heated Temp 10	Heated Temp 11	Heated Temp 12	Heated Temp 13	Heated Temp 14	Heated Temp 15	Adiabatic Temp 1	Adiabatic Temp 2	Adiabatic Temp 3	Adiabatic Temp 4	Adiabatic Temp 5	Adiabatic Temp 6	Adiabatic Temp 7	Adiabatic Temp 8	Adiabatic Temp 9	Adiabatic Temp 10	Adiabatic Temp 11	Adiabatic Temp 12	Adiabatic Temp 13	Adiabatic Temp 14
5.016534799	1.03242907	350.2820768	350.0179405	350.1134725	350.3592386	350.0332831	350.0315863	350.1350461	350.06686	350.2625871	350.2806728	350.0485342	350.0280106	350.2508268	350.0935489	350.1167609	305.0132749	305.0040607	305.0074123	305.001229	305.021415	305.0084717	305.0109231	305.0064364	305.0006056	305.005252	305.0194182	305.0056611	305.0437831	305.0069077
5.018873564	1.039799697	350.4982649	350.4607861	350.246186	350.3746288	350.356785	350.4038274	350.1365837	350.116148	350.4663253	350.4540352	350.2419506	350.1439013	350.2582012	350.2590954	350.1649639	305.0231585	305.0342421	305.0090619	305.006207	305.0621194	305.0198064	305.0408325	305.0080807	305.0017159	305.0512894	305.0357286	305.0195287	305.0456092	305.0149299
5.097472411	1.079699319	350.5354015	350.6960772	350.3220395	350.7415652	350.7779902	350.7782405	350.2860264	350.3651885	350.6075712	350.8037462	350.2537782	350.3053518	350.7528062	350.3364145	350.2369547	305.0410894	305.0418905	305.0635271	305.0264031	305.1052949	305.0361619	305.041018	305.0508925	305.008733	305.0942556	305.0412917	305.0396644	305.0461499	305.0560911
5.135616252	1.081619141	350.6586428	350.8824967	350.6554973	351.2482624	351.0805241	351.3482797	350.4684166	350.519305	350.7461204	351.1529225	350.2845205	350.3226528	350.8184591	350.4341861	350.3114024	305.0527227	305.0427986	305.0793734	305.0268759	305.1479183	305.042709	305.0457191	305.070721	305.024441	305.1019442	305.0462698	305.0673204	305.1128298	305.061961
5.166720123	1.096013111	351.0532736	351.2137058	350.6691632	351.4610413	351.2875124	351.5474146	350.9417484	351.0228279	350.7594638	351.4021934	350.4466302	350.4395786	350.8185695	350.6189808	350.3143206	305.0584262	305.0620248	305.0840238	305.0389032	305.1524894	305.0470537	305.0836138	305.1169392	305.0284589	305.1155197	305.0493225	305.0779605	305.1254963	305.0688911

Table 1 – Model Thermocouples Temperature data

Power Input (W)	Air Velocity (m/s)	Reynolds Number	Nusselt Number	Convective Heat Loss (Qcv, W)	Radiative Heat Loss (Qrd, W)	Richardson Number
5.016534799	1.03242907	10267.25042	27.14510249	3.93204482	1.084489979	0.276882778
5.018873564	1.039799697	10340.54948	27.0417193	3.929887686	1.088985878	0.273864591
5.097472411	1.079699319	10737.3413	27.42545071	4.002648633	1.094823778	0.255080617
5.135616252	1.081619141	10756.43345	27.53320948	4.034986527	1.100629725	0.255226603
5.166720123	1.096013111	10899.5779	27.59509363	4.060343513	1.10637661	0.249567958
5.173982664	1.108628221	11025.03204	27.53059044	4.063185491	1.110797173	0.244663218
5.187278987	1.122530483	11163.28657	27.52527602	4.072996116	1.114282872	0.239262946
5.226504303	1.135712547	11294.37892	27.6352319	4.10626841	1.120235893	0.23471281
5.295910516	1.150889299	11445.30794	27.99961932	4.171876523	1.124033993	0.229193151
5.329721689	1.155870281	11494.84258	28.13978714	4.202451618	1.127270072	0.227747248
5.373033684	1.162658566	11562.35038	28.28510258	4.240250005	1.13278368	0.225953323
5.403811992	1.199964693	11933.35054	28.33194347	4.264885969	1.138926023	0.213001931
5.415209044	1.215814196	12090.96991	28.22651736	4.269100143	1.146108901	0.208465429
5.422597697	1.239681155	12328.32088	28.14857772	4.271578626	1.15101907	0.201187674
5.44321868	1.245737487	12388.54959	28.15997902	4.287421752	1.155796928	0.199894218
5.448601257	1.24878724	12418.87863	28.04671401	4.286920536	1.161680721	0.199699033
5.486020596	1.250289684	12433.82006	28.17978754	4.319951913	1.166068683	0.199806366
5.518953163	1.257367549	12504.20767	28.30087197	4.349244092	1.169709071	0.198051844
5.627161185	1.273157155	12661.23137	28.88460818	4.452893473	1.174267713	0.193776548
5.655172289	1.293475396	12863.29123	28.90778093	4.47464831	1.180523979	0.188502549
5.656709761	1.342101213	13346.86289	28.83274052	4.473077112	1.183632649	0.175484734
5.671132792	1.345731125	13382.96146	28.82080341	4.483405394	1.187727398	0.17501479
5.730544632	1.350464838	13430.03706	29.03550566	4.536159236	1.194385397	0.174534688
5.769735201	1.350773132	13433.10297	29.16876251	4.570710361	1.19902484	0.174980756
5.788366608	1.355040277	13475.53866	29.12237272	4.582731494	1.205635114	0.17461545
5.803368869	1.35948571	13519.74739	29.08246839	4.592427104	1.210941765	0.174080903
5.830021229	1.385680004	13780.24313	29.13181375	4.614270073	1.215751156	0.168073407
5.979937285	1.409573893	14017.86192	29.98975499	4.760711575	1.21922571	0.16278436
6.026002059	1.428229591	14203.3882	30.16526681	4.802300637	1.223701422	0.159014065
6.0705849	1.432365743	14244.5212	30.33429965	4.842620084	1.227964815	0.158536036
6.084433671	1.460647167	14525.77293	30.263208	4.85018128	1.234252391	0.153052979
6.103665061	1.49006681	14818.34397	30.31206063	4.866728035	1.236937026	0.147332837
6.191227283	1.499355112	14910.71382	30.75348491	4.950264642	1.240962641	0.145886294
6.412548154	1.53206002	15235.956	32.00034772	5.166583142	1.245965011	0.140147897
6.431276457	1.54692577	15383.79219	32.00528713	5.181113316	1.250163141	0.137832563
6.469311536	1.571863021	15631.78695	32.14230951	5.215357217	1.253954319	0.133803356
6.500416025	1.604047249	15951.85109	32.2248497	5.24226107	1.258154955	0.128819868
6.545970476	1.614660955	16057.40176	32.35991773	5.282355942	1.263614534	0.127569539
6.613932771	1.61516726	16062.43684	32.63101556	5.344637199	1.269295572	0.127921061
6.641271416	1.626021226	16170.37684	32.69221449	5.368050492	1.273220924	0.126534587
6.64823271	1.653822345	16446.85205	32.60176583	5.369812495	1.278420215	0.122695803
6.718854248	1.661389233	16522.10287	32.94819059	5.437288867	1.281565381	0.121814075
6.80260205	1.701154853	16917.56208	33.29645813	5.514872545	1.287729505	0.116610904
6.821509901	1.704464009	16950.4708	33.31269126	5.529964598	1.291545302	0.116419674
6.864838952	1.707551937	16981.17948	33.48965658	5.570240282	1.294598669	0.116226407
6.90774543	1.717017142	17075.3086	33.63837643	5.608943713	1.298801716	0.115235479
6.927493194	1.721125559	17116.16578	33.6320044	5.623899841	1.303593352	0.115013584
6.959354167	1.737147374	17275.49875	33.66830177	5.649751585	1.309602582	0.113298519
7.06902502	1.741936806	17323.12846	34.20775052	5.755140951	1.313884069	0.112968165
7.129038638	1.743512996	17338.80327	34.44319416	5.810519863	1.318518776	0.113070838
7.137211639	1.762415069	17526.77969	34.42943912	5.816483323	1.320728316	0.110816279
7.146314262	1.766663194	17569.02623	34.33733681	5.819858979	1.326455283	0.11064397
7.190329843	1.798621464	17886.84329	34.44169326	5.857677707	1.332652135	0.107115139
7.254642258	1.811151575	18011.45213	34.74197069	5.919196651	1.335445607	0.105824967
7.264357495	1.829269755	18191.63292	34.69005327	5.924777577	1.339579918	0.103992255
7.270752206	1.85304262	18428.04815	34.61686731	5.927046743	1.343705463	0.101594265
7.300755643	1.854633295	18443.86703	34.69240918	5.953173163	1.34758248	0.101645316
7.318751075	1.884277819	18738.67444	34.63954631	5.965147092	1.353603983	0.098820833
7.319664784	1.896104188	18856.28475	34.55717461	5.962691884	1.3569729	0.097784308
7.372050622	1.915395387	19048.13092	34.72341591	6.009682189	1.362368433	0.09611731
7.452770798	1.928220896	19175.67742	34.9773954	6.08184613	1.370924668	0.09528484
7.492229813	1.934064412	19233.78973	35.08277882	6.116501471	1.375728341	0.094963486
7.524100822	1.936590305	19258.90911	35.1819851	6.145150209	1.378950613	0.09489123
7.55168895	1.962666602	19518.2314	35.18135823	6.166266929	1.385422021	0.092705622
7.688167646	1.963410191	19525.62621	35.84821153	6.298380766	1.38978688	0.092860016
7.746871585	1.977535725	19666.10114	36.07524306	6.352803015	1.39406857	0.091748055
7.767943669	2.01294994	20018.28669	36.04811918	6.368013827	1.399929842	0.088826972
7.768938714	2.03993029	20286.59957	35.95387171	6.36509154	1.403847174	0.086679771
7.774428257	2.052483485	20411.43797	35.82355488	6.364130932	1.410297325	0.085921233
7.788792694	2.065659205	20542.46723	35.76458395	6.372841684	1.41595101	0.085084809
7.80817728	2.071708692	20602.62788	35.76207159	6.387738589	1.420438691	0.084792318
7.808618357	2.0841157	20726.01248	35.63358419	6.382767802	1.425850556	0.084022443
7.822172587	2.120654808	21089.38483	35.54173183	6.389383585	1.432789002	0.081446014
7.845836562	2.141038233	21292.09292	35.5752704	6.409032388	1.436804174	0.080072766
7.856004657	2.152576206	21406.8352	35.48760861	6.413394892	1.442609765	0.07946641
7.87976841	2.159675284	21477.43376	35.49536247	6.432010813	1.447757597	0.079156695
7.97517402	2.181924674	21698.69842	35.91563627	6.523068344	1.452105676	0.07772814
7.987776127	2.18747231	21753.86828	35.81504783	6.528536256	1.459239871	0.077616593
7.995109119	2.19355004	21814.30979	35.71714326	6.530075725	1.465033394	0.077416909
8.088845265	2.24050457	22281.26092	36.17054189	6.621488784	1.467356481	0.074301637
8.099267522	2.274730015	22621.62446	36.13877056	6.628296217	1.470971305	0.072220125
8.150852801	2.276140869	22635.65505	36.25576401	6.672911101	1.4779417	0.072381807
8.178106835	2.306684319	22939.40207	36.23064345	6.692732101	1.485374735	0.070735998
8.194066448	2.316104588	23033.0843	36.21778061	6.704482014	1.489584434	0.0703099
8.210761804	2.318632577	23058.22452	36.19059464	6.716195316	1.494566488	0.07033203
8.214261945	2.333748321	23208.54684	36.07345292	6.713910974	1.500350971	0.069625647
8.216957624	2.336450482	23235.41916	35.98845931	6.712376299	1.504581325	0.069612831
8.316167308	2.337295669	23243.82433	36.38691231	6.805905472	1.510261836	0.069759413
8.325674689	2.407515463	23942.14272	36.33204475	6.810906062	1.514768626	0.065897099
8.336601744	2.415416239	24020.71398	36.29686809	6.817858945	1.5187428	0.065597051
8.474260193	2.456886652	24433.12692	36.93537892	6.951629506	1.522630686	0.063527715
8.487548186	2.489799388	24760.4359	36.90533303	6.96077596	1.526772227	0.061991085
8.493449226	2.505852843	24920.08352	36.85514187	6.963260053	1.530189173	0.061304566
8.524100709	2.524189808	25102.44008	36.9464011	6.990937713	1.533162996	0.060507428
8.861502697	2.54349481	25294.42353	38.60371954	7.323033261	1.538469436	0.059743349
8.923985122	2.573843953	25596.23821	38.81805276	7.38077455	1.543210572	0.058478091
8.930337326	2.611758293	25973.28689	38.74946324	7.382918399	1.547418927	0.056909639
8.954367515	2.626625394	26121.13651	38.75137372	7.401638333	1.552729183	0.056407117
9.113736974	2.629354209	26148.2739	39.46689023	7.556099911	1.557637063	0.056422979
9.132511146	2.650171173	26355.29343	39.43586293	7.569385198	1.563125948	0.055681487
9.194377754	2.650757582	26361.12513	39.64361273	7.626458442	1.567919312	0.055782642
9.327053144	2.653307384	26386.48227	40.22616941	7.754777996	1.572275148	0.055792392
9.373734551	2.656767162	26420.88891	40.30605076	7.794740861	1.57899369	0.055823089
9.39583419	2.666022182	26512.92777	40.27156584	7.810556015	1.585278175	0.055596229
9.47015575	2.685817965	26709.79192	40.5433054	7.880313583	1.589842167	0.054898518
9.558930487	2.70030486	26853.86049	40.90204351	7.965112787	1.593817699	0.054414012
9.640031033	2.712707361	26977.20028	41.21525349	8.04203616	1.597994873	0.054024602
9.640422277	2.765230709	27499.53192	41.07213833	8.036509146	1.603913131	0.052137092
9.649577979	2.766639259	27513.53959	40.99125411	8.040406313	1.609171666	0.052212097
9.71164426	2.778388815	27630.38601	41.10036273	8.093698741	1.617945519	0.051976228
9.776029865	2.784881963	27694.95875	41.32741721	8.153964467	1.622065398	0.051833005
9.780596185	2.810788989	27952.59768	41.19045505	8.151657701	1.628938484	0.051036664
9.781120726	2.901053519	28850.25599	41.05661815	8.14638653	1.634734196	0.048035219
9.78159581	2.906414096	28903.5656	40.92187516	8.141050652	1.640545158	0.047984323
9.828737828	2.937784523	29215.5367	41.04251488	8.183334691	1.645403137	0.047070184
9.853851318	2.938528256	29222.93294	41.01193182	8.201719884	1.652131434	0.047187219
9.874187962	2.943321286	29270.59842	41.04844907	8.219468607	1.654719355	0.04709351
9.911586705	2.970563316	29541.51364	41.12068981	8.252072172	1.659514533	0.04633556
9.947963671	2.973763245	29573.33614	41.15896205	8.282200591	1.66576308	0.046361553
9.99743769	2.978159561	29617.05641	41.28152632	8.326290318	1.671147372	0.04633288

Table 2 – Model Result Data

6.2 Assumed Values:

$\in = 0.15,\ \sigma = 5.67 * 10^{-8},\ surface\ area = 0.02,\ k = 0.026,\ L = 0.18,\ \mu = 1.81 * 10^{-5}, g = 9.81$

6.3 Predicted Graphs

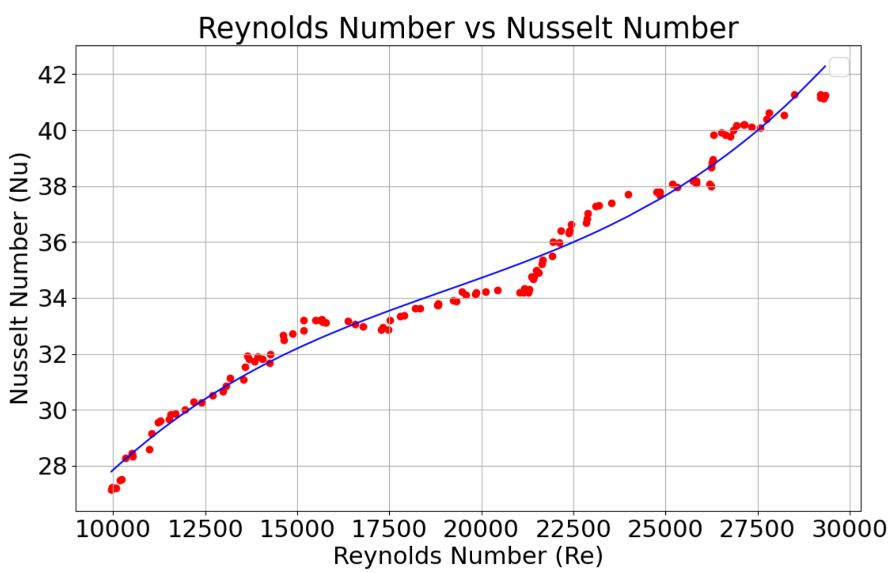

Figure 4

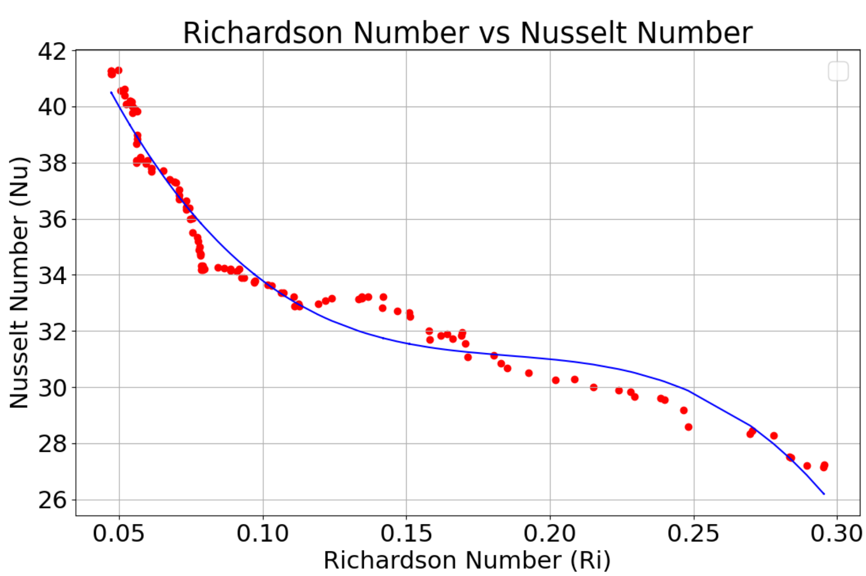

Figure 5

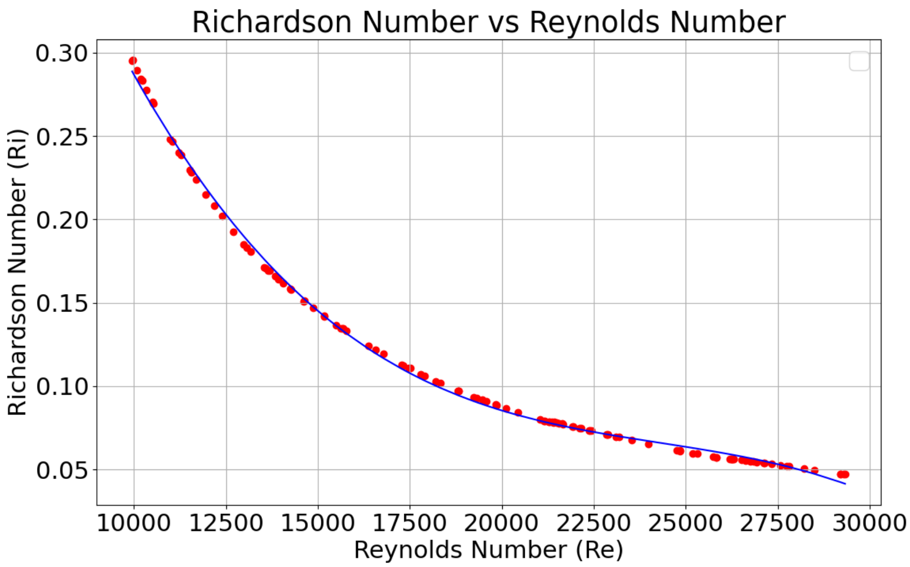

Figure 6

7. References

[i] *A. Rajiand M. Hasnaoui, Combined mixed convection and radiation in ventilated cavities, Eng. Comput. 18 (2001) 922–949.*

[ii] *A. Bahlaoui, A. Raji, M. Hasnaoui, C. Ouardi, M. Naïmi, T. Makayssi, Height partition effect on combined mixed convection and surface radiation in a vented rectangular cavity, J. Appl. Fluid Mech. (2011) 89–96.*

[iii] *S. Venkatachalapathy, M. Udayakumar, Experimental and numerical investigation of mixed-convection heat transfer from protruding heat sources in an enclosure, Exp. Heat Tran. 25 (2) (2012) 92–110.*

[iv] *M. Belmiloud, A. Sad, N. Chemloul, M.B. Guemmour, Effect of baffle length on mixed convection coupled to surface radiation in a rectangle cavity, Revue des Energies Renouvelables 20 (2017) 81–89.*

[v] *H. Doghmi, B. Abourida, L. Belarche, M. Sannad, M. Ouzaouit, Numerical study of mixed convection inside a three-dimensional ventilated cavity in the presence of an isothermal heating block, Int. J. Heat Technol. 36 (2018) 447–456.*

[vi] *Ravi Shankar Prasad, S.N. Singh, Kumar Gupta Amit, Combined laminar natural convection and surface radiation in top open cavities with right side opening, J. Eng. Sci. Technol. 14 (1) (2019) 387–410.*

[vii] *Om Prakash, S.N. Singh, *Experimental and numerical study of mixed convection with surface radiation heat transfer in an air-filled ventilated cavity*, *International Journal of Thermal Sciences*, Volume 171, 2022, 107169, ISSN 1290-0729.*